Egypt. J. Chem. **Vol. 67,** No. 2 pp.615 - 623 (2024)

Egyptian Journal of Chemistry

http://ejchem.journals.ekb.eg/

Development and Evaluation of Pectin extracted from Citrus sinensis peel and micro/nanocellulose from the solid fraction of citrus wastes.

Sara ZA. Mahdy[a], Alaa S. Amin [a], Ragab Abouzeid[b], Islam M. I. Moustafa[a], Ahmed M. Youssef[c], El Sayed El Habbasha[d]

[a] *Chemistry Department, Faculty of Science, Benha university, Cairo, Egypt.*

[b] *Cellulose and paper Department, National Research Centre, Cairo, Egypt, P.O. 12622*

[c] *Packaging Materials Department, National Research Centre, 33 El Bohouth St. (former El Tahrir St.), Dokki, Giza, P.O. 12622, Egypt.*

[d] *Field crops Research Department., National Research Centre, Cairo, Egypt, P.O. 12622*

Abstract

Pectin, a biopolymer that occurs naturally in plants, has a wide range of applications in various industries. The aim of the current study is to extract pectin through acid hydrolysis using sulfuric acid from orange waste, also extraction of micro/nanocellulose from the solid fraction of citrus wastes. Investigate the effects of multiple variables such as temperature, time and pH to reach the optimum conditions for the highest pectin yield. The extracted pectin and micro/nanocellulose were characterized using FTIR, XRD, TEM, scanning electron microscope and determination of the degree of esterification of pectin. It was found through our study that different parameters such as temperature, pH and time effect on the pectin yield, where temperature (80, 90, 100) °C , time (60, 90, 120) min and pH (from 1.5-2.0), So we found that the pectin yield at its best result was 16.9 %, At which (temp 90 °C ,time 90 min, pH 1.5). Determination of degree of esterification of extracted pectin recorded 83 which is suitable value.

Keywords: Extraction of pectin, Extraction of micro/nanocellulose, FTIR, XRD, SEM, TEM, Determination of degree of Esterification.

1. Introduction

Recent years have seen significant interest in biomaterials as they are emerging as a viable solution to the world's dire needs, including the rapid depletion of non-renewable resources, global warming, and environmental pollution. Among the numerous renewable materials available today, plant-derived biomass (lignocellulosic biomass, starch, gum), animal-derived materials (chitin, chitosan, gelatin) and microbe-derived materials (alginates, bacterial cellulose, polyhydroxyalkanoates) have frequently been cited as promising candidates due to their ample supply and environmental friendliness. Pectin is a natural substance that is present within the cellular structure of most plants. It has a rich history of applications due to its gelling, thickening, and stabilizing properties, finding uses in a wide array of industries, including food, pharmaceuticals, and cosmetics. In the production of orange juice, after the oranges are squeezed, a significant amount of orange peel is often left unused. Some farmers may consider this peel as waste and use it as cattle feed or fertilizer. However, this orange peel can serve as the raw material for our process. By extracting pectin from the orange peel, we can turn what was once considered waste into a valuable product that can be sold. This not only reduces waste but also adds value to the orange peel, serving a more meaningful purpose [1].

The most popular sources of commercially available pectin are apple pomace, citrus, and orange peels. However, the pectin produced from these sources varies slightly, making each one more suitable for certain applications. Additionally, sugar beet and sunflower seed head residues have been used as alternative sources of pectin. In the food industry, high methoxyl pectin has multiple uses such as gelling, stabilizing, emulsifying, and thickening, while low methoxyl pectin is mainly utilized as a fat replacer in products like ice cream, spreads, and low-

*Corresponding author e-mail: sarazain5566@gmail.com.; (Sara ZA. Mahdy).

Receive Date: 31 August 2023, Revise Date: 24 October 2023, Accept Date: 24 October 2023

DOI: 10.21608/EJCHEM.2023.232794.8532

calorie beverages [2-4]. In microcrystalline cellulose (MCC), alpha cellulose is partially depolymerized by treatment with mineral acids so that it becomes a fine, white, odorless powder. Most common organic solvents do not dissolve MCC, including water, dilute acids, and alkalis [5]. Compared to other cellulose fibers, it has a lower degree of polymerization and a higher specific surface area [6]. MCC has been widely used especially in pharmaceuticals, cosmetics, food and other industries [7-8]. Researchers were used MCC as starting material for cellulose reinforced nanocomposites [9]. It likewise reported that type of cellulose, its origin and the method of preparation affects the overall properties of MCC [10]. MCC can be used as filler, which produce tablets of high mechanical and physical properties such as high rigidity, fast dissociation time and a high rate of drug release. Furthermore, it is used in production direct pressure tablet. MCC tablets production is growing due to many advantages for examples; uniform particle size, producing more stable tablet and profitable in economical point of view. Also, MCC can decrease sedimentation in suspension and dry syrup [11]. Nanocrystals of cellulose that have rod-like shapes are called cellulose nanocrystals (CNC). A CNC is frequently described as a nanowhisker, a nanocrystalline cellulose crystal, a rod-like cellulose crystal or a nanorod in literature [12-14]. In the CNC preparation, the primary technique employed is strong acid hydrolysis. This method requires the selective removal of the non-crystalline portions of natural cellulose while preserving the integrity of the crystallized segments. Subsequently, a high-intensity mechanical or ultrasonic process is applied, resulting in the formation of truncated, rod-shaped structures following the cellulose hydrolysis. In CNC isolation, concentrated sulfuric acid is commonly used. A negative charge is imparted to nanocrystalline particles in an aqueous medium due to the production of sulphate ester groups during sulfuric acid hydrolysis. As a result, CNCs have very limited flexibility due to their high crystallinity [15-17]. With its large surface area, high specific strength, high modulus, outstanding stability and outstanding optical properties, CNC exhibits a number of unique characteristics. It is well known that CNCs are highly mechanically efficient. Based on theoretical calculations, CNC should have a Young's modulus of 167.5 GPA along its cellulose chain axis. As compared to steel, this modulus is substantially greater than Kevlar. CNCs derived from tunicates exhibit a modulus of 143 GPa; CNCs derived from cotton, on the other hand, have a modulus of 105 GPa [18-19]. In addition, CNCs have an excellent thermal stability up to 260 °C, and a high tensile strength of 9 GPa. A low thermal expansion coefficient of 0.1 ppm/K and a low density of 1.5-1.6 g/cm3 are other characteristics of these materials. A cellulose nanofiber (CNFs) is a type of nanocellulose produced through the griding of cellulose fibers by means of mechanical treatment. CNFs were initially successfully synthesized in 1982 by Turbak et al. using high-speed homogenization of eucalyptus pulp [20].

Cellulose nanofibers (CNFs) are characterized by their remarkable features: high aspect ratios, nanoscale dimensions, and lengths that can extend to several microns. These fibers have been referred to by various names, such as microfibrillated cellulose, cellulose nanofibers, and nanocellulose fibers. In contrast to cellulose nanocrystals (CNC), CNFs are pliable, elongated fibers encompassing both amorphous and crystalline segments, and they are produced through mechanical disintegration of cellulose fibers. It has been observed that chemically pretreating cellulose fibers can substantially reduce energy consumption by as much as 98 percent [21]. Effective pretreatment of cellulose fibers expedites the disruption of hydrogen bonds, alters crystallinity, and increases the accessibility of hydroxyl groups, thereby enhancing fiber reactivity [22]. Since cellulose fibrillation necessitates a liquid medium, the resulting product must be preserved as a dispersion because CNFs establish irreversible hydrogen bonds with each other after drying [23]. Alternatively, coupling agents or TEMPO can be employed to oxidize surface hydroxyl groups, forming aldehyde or carboxyl groups, and introducing a surface charge can also reduce the cohesion between fibers [24–27]. The goal of this work is to take the orange peel and extract pectin from it by acid hydrolysis, which is used in the pharmaceutical industries and in food packaging, also extracting cellulose and nano-cellulose such as Microcrystalline Cellulose [MCC], cellulose nanofibers [Tempo-CNF] and cellulose nanocrystals [CNC]. That is meaning we finally get zero waste from the raw material [orange peel]. These nanomaterials have many uses in bio-nanocomposite. The objectives were to characterize the FTIR, XRD, SEM, TEM of the resulting substances, Also determination of degree of esterification of pectin.

2. Materials and Methods [Experimental]

2.1. Materials

Mediterranean Citrus for example orange waste was collected from a local industrial facility in Egypt and cleaned to remove dirt, dust, and pesticide residues. They were cut into little pieces and dried at a temperature of 60 °C until the weight reached a constant value. The other chemicals were analytical grade and used as received.

2.2. Extraction of pectin from orange peel

The orange waste (5 g) will be dispersed in distilled water (250 ml) adjusted in pH with concentrated sulfuric acid to [2.0 or 1.5]. The mixture will be shaken in a thermostatic bath with different temperatures [80-90-100] °C, and then cooled with the pH adjusted to [4.0-4.5] using 2N NaOH. Pectin will be precipitated by using 75% ethanol and then subjected to centrifugation at 5000 rpm before being dried [28].

2.3. Isolation of Cellulose from pectin Extraction Residue

The procedure involves collecting the pulp waste after pectin extraction and washing with hot water to remove organic materials and sugars, followed by a 12 h drying at 105 °C. Lignin residue will then be removed through the chlorite method, in brief, 5 g of pulps will be heated at 70-80 °C for 1 hour with 80 ml of distilled water containing 1.5 g of sodium chlorite and 1 ml of glacial acetic acid drops. This step will be repeated twice, and the pulps will be filtered and washed with distilled water until they achieve a neutral pH. The resulting holocellulose was determined and dried for subsequent utilization [29].

2.4. Microcrystalline Cellulose Preparation

Cellulose extracted from citrus wastes was hydrolyzed using sulfuric acid (2 M). The hydrolysis conditions used were by refluxing citrus wastes in 2 M sulfuric acid solution for 45 min in a liquid ratio of [1:10]. The hydrolyzed pulps were then washed with distilled water and acetone, followed by drying in air till constant weight. The yield was about 30 % based on the weight of citrus wastes [30].

2.5. Preparation of TEMPO-cellulose nanofibers

Following the method outlined in our prior works [6-7], 10 g of cellulose fiber will be suspended in 750 ml of water containing 0.025 g of TEMPO and 0.25 g of sodium bromide in order to undergo the oxidation process necessary for the production of surface functionalized CNFs. The slurry will be continuously agitated while NaClO solution (3.84 mmol/g of cellulose) is added. At room temperature, the pH will be maintained at 10.5 with the addition of 0.5 M NaOH for all experiment. Then, hydrochloric acid will be used to halt the process and return the pH to neutral (HCl). After collecting the pulp, it will be rinsed in deionized water before being homogenized to create carboxyl-functionalized CNFs. The resulting pulp will be rinsed with deionized water before being homogenized to create functionalized CNFs with carboxylic groups. As a result, charged carboxylate groups are formed on the surface of the fiber for this treatment. As a result of the repulsion between the negatively charged carboxylate groups, the C6 hydroxyl group is selectively changed into a carboxylate group, and the nanofibers detach from the fibers. A 1-2% fiber suspension in water will be homogenized with a high-pressure homogenizer after oxidation pretreatment of produced fibers.

2.6. Preparation of cellulose nanocrystals (CNC)

Isolating cellulose nanocrystals from bleached pulp via acid hydrolysis at 45 °C for 45 min with 65% sulfuric acid has been described previously [14-16], to determine the composition of the cellulose nanocrystals, a transmission electron microscope (TEM) JEOL 1230 (Japan) was used with an acceleration voltage of 100 kV. On a copper grid with a carbon coating, a drop of cellulose nanocrystals suspension was employed.

2.7. Characterization of pectin and micro/nanocellulose

2.7.1. Determination of degree of esterification (DE) of pectin

The degree of pectin esterification will be assessed following the procedure outlined by Dominiak et al. In a nutshell, 0.2 g of pectin will be dissolved in 100 ml of deionized water and subjected to titration using 0.1 M NaOH with phenolphthalein as the indicator. The volume of 0.1 M NaOH used in this titration will be recorded as V1. Subsequently, the same sample will undergo saponification through the addition of 10 ml of 1 M NaOH, followed by 15 min of stirring. Afterward, 10 ml of 1 M HCl will be introduced into the sample, and the mixture will undergo another titration with 0.1 M NaOH until a color change is observed, recording the volume as V2 [31].

The DE will be calculated according to the formula in equation (2):

$$DE = (V2/ (V2+V1)) \times 100$$

Figure [1] Mechanism of determination of degree of esterification of pectin

2.7.2. Infrared (IR) spectral analysis

Fourier transform infrared (FTIR) spectroscopy was used to characterize the functional group composition of pectin and the prepared microcrystalline Cellulose [MCC], TEMPO-cellulose nanofibers [CNF] and cellulose nanocrystals [CNC]. They were recorded in the range of 400–4000 cm^{-1} on (Shimadzu 8400S) FT-IR Spectrophotometer, With 4 cm^{-1} resolution, for each sample. The positions of significant transmittance peaks at a particular wavenumber were tracked.

2.7.3. Transmission electron microscopy (TEM)

To study the structure and surface morphology of the pectin as well as the prepared microcrystalline Cellulose [MCC], TEMPO-cellulose nanofibers [CNF] and cellulose nanocrystals [CNC], a JEOL JEM-1230 transmission electron microscope (TEM) with an acceleration voltage of around 80 kV was utilized. The microscopy probes were prepared by placing a drop of the emulsion of the polymer material onto a Lacey carbon coated copper grid. Subsequently, the grid was allowed to dry in air, followed by a high vacuum.

2.7.4. Scanning electron microscopy (SEM)

The morphology of pectin as well as the prepared microcrystalline Cellulose [MCC], TEMPO-cellulose nanofibers [CNF] and cellulose nanocrystals [CNC] were detected using a scanning electron microscopy (SEM) (High Resolution Quanta FEG 250-SEM, Czech Republic) at different magnifications. In order to, investigate the filler dispersion and the compatibility between polymer and filler. The surfaces of the samples were examined without coated gold and at low vacuum.

2.7.5. X-ray diffraction (XRD)

A Philips X-ray diffractometer was used to analyze the crystal structure of pectin filler powders, as well as microcrystalline Cellulose (MCC), TEMPO-cellulose nanofibers (CNF) and cellulose nanocrystals (CNC). The equipment was set at 45 kV, 40 mA, with a wavelength of 0.15418 nm, and diffraction scans were conducted over a 2θ range of 5 to 80° with a step size of 0.02 and a step time of 1s.

3. Results and discussion

3.1. FTIR- Fourier transforms infrared

3.1.1. FTIR of Pectin extracted

Figure 2 (A, B, and C) displays the FTIR spectra of pectin samples with varying degrees of acetylation, revealing comparable characteristics among them. The FTIR spectrum of pectin exhibits distinct peaks at specific wavenumbers. At 3433 cm^{-1}, a peak corresponds to the stretching vibrations of hydroxyl groups, while at 2938 cm^{-1}, another peak represents the stretching vibrations of methyl ester groups or C-H bonds of pyranoid ring carbons. A vibration at 1748 cm^{-1} corresponds to the stretching vibration of carboxyl groups, and at 1614 cm^{-1}, there is a stretching vibration indicating the presence of carboxyl and methyl ester moieties. The region from 1440 to 1237 cm^{-1} predominantly encompasses the stretching vibrations of -C-O-C- bonds and -CH groups. Furthermore, the polysaccharide "fingerprint" region within the range of 1210-1001 cm^{-1} corresponds to vibration bands associated with glycosidic bonds and pyranoid rings of the pectin structure [3, 32].

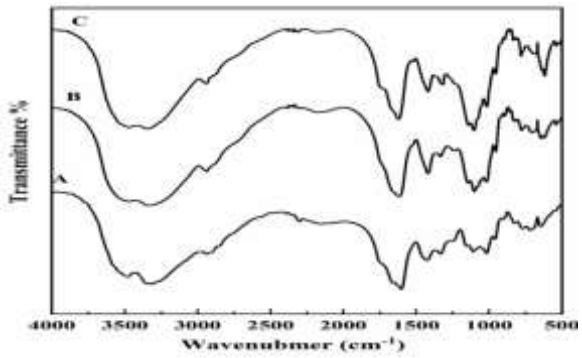

Figure [2] FT-IR of extracted pectin with different degree of acetylation

3.1.2. FTIR of extracted cellulose, nanocellulose (CNC and CNF)

Figure [3] displays the FTIR spectra of extracted cellulose, CNC (Cellulose Nanocrystals), and TEMPO-CNF (TEMPO-Oxidized Cellulose Nanofibers). It indicates that absorption bands at 3200-3300 cm^{-1} indicate O-H stretching vibrations in hydrogen bonds, whereas peaks around 1600-1640 cm^{-1} represent O-H bending in absorbed water. The absorption peaks about 2900 cm^{-1} reflect the aliphatic C- H stretching vibrations of all polysaccharide hydrocarbon components. The C-H stretching peak intensity of MCC was somewhat lower than that of cellulose, indicating that the bleaching process removed both lignin and hemicellulose. MCC spectra no longer show an absorption peak at 1236 cm^{-1}, showing the C-O stretching of lignin's aryl group. This indicates that lignin is being chemically removed from the OP surface in a limited capacity. The alkaline treatment destroyed both lignin and hemicellulose, which are generally present in cellulose, as demonstrated by the disappearance of the two peaks in the MCC spectra. Furthermore, the MCC spectra around 1425-1428 cm^{-1} show CH_2 symmetric bending, and the peak at 896 cm^{-1} is caused by stretching of the glycosidic connections between the cellulose, while the peaks around 1160 cm^{-1} are caused by C-O-C asymmetrical ring stretching.

3.1.3. FTIR of TEMPO oxidized cellulose nanofibers [T-CNFs].

The effect of different pretreatments on cellulose fibrillation can be determined using FTIR. FTIR of T-CNF's spectrum is depicted in Figure 3. This study discovered that CNF has a distinct peak around 3300 cm^{-1}, which is attributed to cellulose's OH group stretching. C-H stretching vibrations have a peak at 2800 cm^{-1}, and C-O stretching vibrations have a peak between 1600 and 1650 cm^{-1}. T-CNFs exhibit their

characteristic C=O band at 1740 cm^{-1} because of TEMPO oxidation.

3.1.4. FTIR of CNCs

FTIR spectroscopy was used to characterize the chemical structure of CNCs, as illustrated in Figure 3. The O-H stretching and C-H stretching vibration modes are represented by the broad band at 3428 cm^{-1} and the peak at 2924 cm^{-1}, respectively. Furthermore, the peak at 1638 cm^{-1} is due to the presence of adsorbed water molecules on the surface of the CNCs; peaks at 1200-1000 cm^{-1} are due to the stretching vibration of C-O for glycosidic bonds and C-O of primary and secondary hydroxyl groups; and a peak at 850 m^{-1} is due to out-of-plane deformational vibration of O-H groups [33-34].

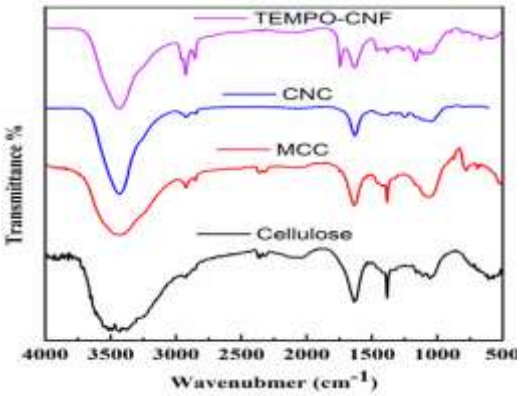

Figure [3] FTIR of extracted cellulose, CNC, TEMPO-CNF, and MCC.

3.2. Effect of different parameters on pectin yield

The influence of extraction time, pH of solution and temperature on pectin yield extracted from orange peels using sulfuric acid were studied. The yield of pectin from the extractions is shown in Table 1 and Figure [4 and 5] for temperature range from [80 to 100 °C], time from [60 to 120] min and pH [1.5 and 2.0]. The percentage yield of pectin at 1.5 pH for 60 min and at temperature 80, 90 and 100 °C are 14.9, 14.1 and 14.8 % respectively. At 1.5 pH for 90 min and at temperature 80, 90 and 100 °C are 15.3, 16.9 and 17.9 % respectively. Likewise at 1.5 pH for 120 min, at temperature 80, 90 and 100 °C the percent yield is 17.0, 15.7and 14.8 percent respectively. It was shown that at pH 1.5, the yield of pectin increased with increasing the temperature. The percentage yield of pectin extracted from orange peels at 2.0 pH for 60 min. at temperature 80, 90 and 100°C was 13.9, 14.2 and 12.4 percent respectively. At 2.0 pH for 90 min and at temperature 80, 90 and 100°C are 12.7, 13.4 and 12.8 percent correspondingly. Likewise at 2.0 pH for 120 min. at temperature 80, 90 and 100°C the percent yield is 12.3, 13.0 and 11.1 percent respectively. At 2.0 pH the effect on percent pectin yield were lower than the pH 1.5.

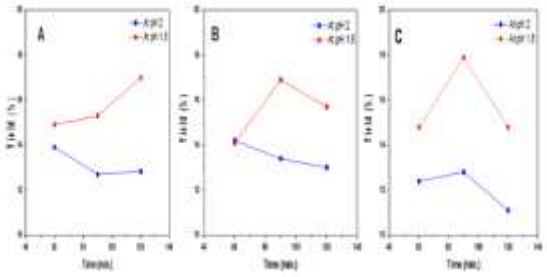

Figure [4] Effect of time on the extraction yield of pectin (A) at 80 °C, (B) at 90 °C and (C) at 100 °C

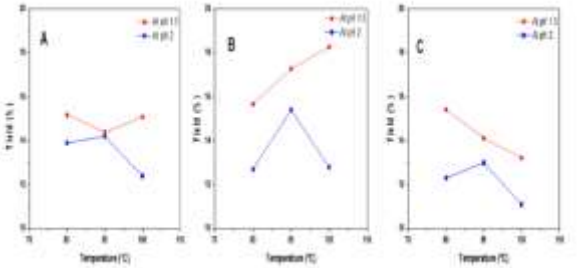

Figure [5] Effects of Temperatures on the extraction yield of pectin (A) at 60 min., (B) at 90 min. and (C) at 120 min.

3.3. Degree of esterification (DE)

The degree of esterification of pectin isolated from orange peel powder with sulfuric acid was found to range between 40 and 91 percent. As the plant became older, the degree of esterification reduced. The reduced DE could be due to the conversion of pectin's to protopectin, which raises sugar levels and softens the fruit during maturation. DE is dependent on species, tissue, and maturity stages [4].

Table 1: Pectin yield with applying different conditions of pH, Time and Temperature, with degree of esterification (DE)

Samples	Temperature (°C)	Time (min.)	pH	Pectin yield %	DE
1	80	60	2.0	13,9	66
2	80	90	2.0	12,7	91
3	80	120	2.0	12,3	85
4	80	60	1.5	14,9	44
5	80	90	1.5	15,3	66
6	80	120	1.5	17	88
7	90	60	2.0	14,2	75
8	90	90	2.0	13,4	82
9	90	120	2.0	13	40

10	90	60	1.5	14,1	63
11	90	90	1.5	16,9	83
12	90	120	1.5	15,7	55.5
13	100	60	2.0	12,4	70
14	100	90	2.0	12,8	70
15	100	120	2.0	11,1	80
16	100	60	1.5	14,8	96
17	100	90	1.5	17,9	81
18	100	120	1.5	14,8	91

3.4. X-ray diffraction [XRD]

3.4.1. XRD for pectin

X-ray diffractogram of prepared pectin is shown in the figure [6].Pectin shows crystalline peaks in its diffractogram at 2θ equal to 9.5, 11.5, 20.8 28.9, 30.9, and 31.5°, which indicates that it is crystalline.

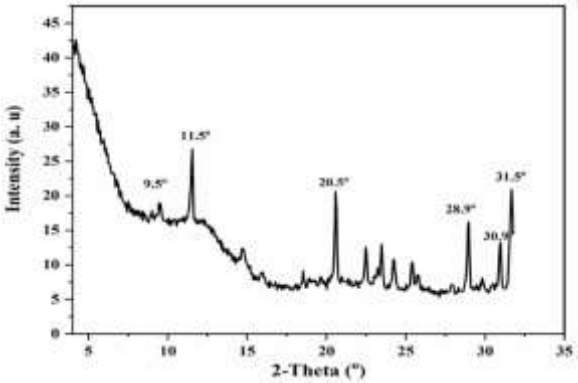

Figure [6] x-ray diffraction of pectin

3.4.2. XRD of MCC, nanocellulose (CNF) and CNC.

X-ray diffraction (XRD) is an analytical technique which is employed to identify crystalline solids and extract information regarding the chemical composition and crystallographic structure. It is based on the principle of diffraction of X-rays, which have wavelengths of a few angstroms, the same as the interatomic distances in crystalline solids. When X-rays interact with the atoms in the crystalline solids, they diffract and form numerous sharp spots known as Bragg diffraction peaks, which provide a unique signature of the material. [35]. X-ray diffraction [XRD] of CNF from Figure [7] shows the wide-angle diffractograms of cellulose nanofibers obtained from citrus wastes. It is typical of semi-crystalline materials to have a broad amorphous peak as well as crystalline peaks on the diffractogram. These peaks were observed at 2 theta angles of 16 °, 22 °, and 34 °, respectively, which are associated with the diffraction planes of (101), (002), and (040). Type 1 cellulose exhibits these peaks. X-ray diffraction [XRD] of CNC was illustrated in figure [7]. The XRD patterns for MCC acquired using H2SO4 shows Peaks at 2θ = 14.7 °; 16.5 ° and 22.5 °, which corresponds to the Iβ cellulose structure that is related to planes (110), (101) and (002), respectively [41]. X-ray diffraction [XRD] of MCC From figure [7], The XRD patterns for MCC obtained using H2SO4 were similar and in accordance with the known diffraction peaks of cellulose with peaks at 2θ angles of 34.5°, 22.5°, and 15.5°, which belong to diffraction from (0 4 0), (0 0 2), and (1 0) planes, respectively [36-37].

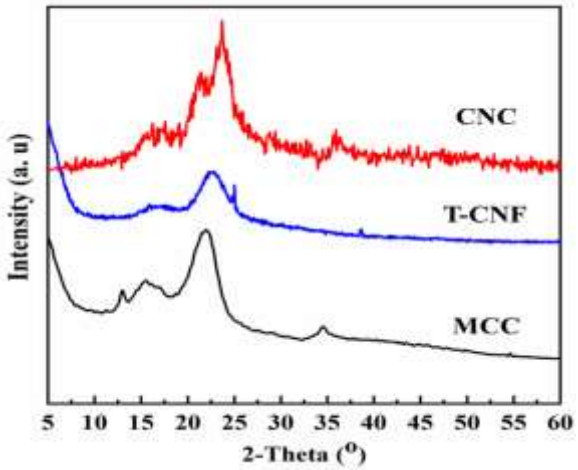

Figure [7] XRD of cellulose and nanocellulose [TEMPO-CNF, MCC, CNC]

3.5. Scanning electron microscopy (SEM)

3.5.1. SEM for pectin

The morphology of isolated pectin by traditional acid hydrolysis was characterized using a Scanning Electron Spectroscopy (SEM). The pectin surface image was taken with different magnifications as shown in Figure [8]. The dried pectin form has crystals in the image of the analysis. This characteristic indicates that pectin has crystalline shape in range of 2.00 kx and 1.00 kx.

Figure [8] scanning electron microscope [SEM] for pectin

3.5.2. SEM for alpha-Cellulose and Microcrystalline cellulose prepared from citrus waste

Fibers of cellulose pulp were obtained after the chemical treatment of biomass, which resulted in the breakdown of lignin and hemicellulose (Figure 9 A, B). After bleaching, the original fiber's surface appeared smooth, suggesting that all traces of lignin had been eliminated. The morphology of the isolated MCC was characterized by SEM and the images at

with different magnifications are shown in Figure 9 (C, D). It can be seen that the drying of the MCC from water resulted in strong aggregation of the particles and the figure at 20 micrometer exhibit long, rod-shaped particles of MCC. As shown in Figure 9 (E, F), SEM was used to examine the morphology of T-CNF. As a result of the oxidation of the native citrus waste cellulose, TEMPO-oxidized fibers have a highly porous surface as compared to native cellulose. There was a continuous irregular mesh of cellulose fibers in the T-CNF, sometimes forming thicker fibers, with thin fibers averaging several hundred nanometers in length. During freeze-drying the T-CNF developed large, interconnected pores of cellulose due to ice growth.

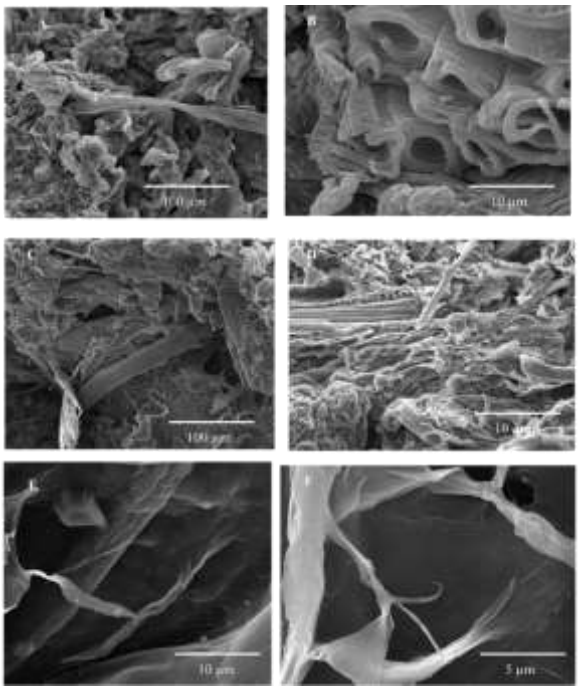

Figure [9] SEM of (A, B) cellulose, (C, D) MCC and (E, F) TEMPO-CNF from citrus wastes

3.6. Transmission electron microscopy (TEM) of T-CNF, and CNC

The morphology of T-CNF was investigated by TEM. Figure 10 (A) shows the range of diameters of nanofiber varied from 3 to 10 nm and having a length varied from nanometers to micrometers. Due to the presence of carboxylate endings on its surface, the T-CNF has a uniform structure, as demonstrated by these data, which are in accordance with our earlier research and confirm this once more [38-39]. The transmission electron microscope of CNCs that were prepared by acid hydrolysis from citrus wastes can be seen in Figure 10 (B). There is no evidence that CNCs have agglomerated into larger structures. Isolated nanocrystals had widths in the range of 4–8 nm and lengths in the range of 60–300 nm. Both dimensions were measured in nanometers. These findings are consistent with those found in previous research described elsewhere [33-40].

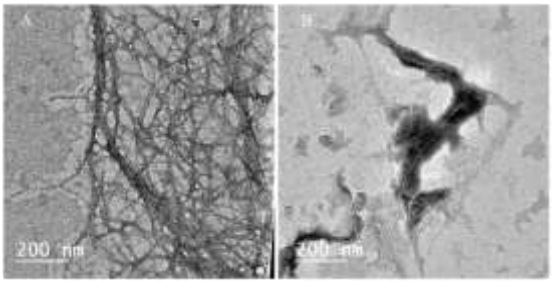

Figure [10] TEM of (A) T-CNFs, and (B) CNC

4. Conclusions

This paper reviewed the preparation of pectin as well as microcrystalline Cellulose, TEMPO-cellulose nanofibers and cellulose nanocrystals extracted from citrus sinensis peel. In addition to their functional properties, pectin extraction methods can directly affect their structural and functional properties. The yield of pectin prepared differs according to different parameters such as temperature, pH and time; also we have reached to optimum condition of extraction which achieves the highest yield. We have made characterization of pectin, microcrystalline Cellulose, TEMPO-cellulose nanofibers and cellulose nanocrystals using FTIR, XRD, SEM and TEM analysis. Therefore, pectin, microcrystalline cellulose, and other materials could be the focus of future research, TEMPO-cellulose nanofibers and cellulose nanocrystals [CNC] extracted from citrus sinensis peel.

5. Conflicts of interest

The authors declare that they have no competing financial interests or personal relationships that could have appeared to influence this work.

6. Formatting of funding sources

There is no funding to report

7. Acknowledgments

The authors gratefully acknowledge Science, Technology and Innovation Funding Authority (STDF), Egypt for funding the MEDISMART project (reference number: PRIMA-EU- 2019-SECTION2) which gave us the opportunity for carried out these experiments and publish this research.

8. References

[1] Quebedeaux B, Bliss F. Horticulture and human health: contributions of oranges and vegetables.

Proc. Symp. 1988. Hort. and Human Health Prentice.
[2] Wargovich M. Anticancer properties of oranges, Hort Science. 2009. 35: 573-575.
[3] A. El-Gendy, R. E. Abou-Zeid, A. Salama, M. A. Diab, and M. El-Sakhawy, Egypt. J. Chem., vol.
[4] Hashmi S.H, Ghatge P, Machewad G.M and Pawar S. 2012. Studies on extraction of essential oil and pectin from sweet orange.Dept. of Food Chem. And Nutrition.
[5] Zhang W, Jia B, Wang Q, Dionysiou D (2015) Visible-light sensitization of TiO2 photocatalysts via wet chemical N-doping for the degradation of dissolved organic compounds in wastewater treatment: a review. Journal of Nanoparticle Research 17:221. https://doi.org/10.1007/s11051-015-3026-1
[6] He F, Ma F, Li T, Li G (2013) Solvothermal synthesis of N-doped TiO2 nanoparticles using different nitrogen sources, and their photocatalytic activity for degradation of benzene. Cuihua Xuebao/Chinese Journal of Catalysis 34:2263–2270. https://doi.org/10.1016/s1872-2067(12)60722-0
[7] Nsor-Atindana J, Chen M, Goff HD, et al (2017) Functionality and nutritional aspects of microcrystalline cellulose in food. Carbohydrate Polymers 172:159–174
[8] Kian LK, Jawaid M, Ariffin H, Alothman OY (2017) Isolation and characterization of microcrystalline cellulose from roselle fibers. International Journal of Biological Macromolecules 103:931–940. https://doi.org/10.1016/j.ijbiomac.2017.05.135
[9] Mathew AP, Oksman K, Sain M (2005) Mechanical properties of biodegradable composites from poly lactic acid (PLA) and microcrystalline cellulose (MCC). Journal of Applied Polymer Science 97:2014–2025. https://doi.org/10.1002/app.21779
[10] Lee SY, Mohan DJ, Kang IA, et al (2009) Nanocellulose reinforced PVA composite films: Effects of acid treatment and filler loading. Fibers and Polymers 10:77–82. https://doi.org/10.1007/s12221-009-0077-x
[11] Kharismi RRAY, Sutriyo, Suryadi H (2018) Preparation and characterization of microcrystalline cellulose produced from betung bamboo (dendrocalamus asper) through acid hydrolysis. Journal of Young Pharmacists 10:s79–s83. https://doi.org/10.5530/jyp.2018.2s.15
[12] Du H, Liu W, Zhang M, et al (2019) Cellulose nanocrystals and cellulose nanofibrils based hydrogels for biomedical applications. Carbohydrate Polymers 209:130–144
[13] Zhang B, Huang C, Zhao H, et al (2019) Eects of cellulose nanocrystals and cellulose nanofibers on the structure and properties of polyhydroxybutyrate nanocomposites. Polymers 11:. https://doi.org/10.3390/polym11122063
[14] Abou-Zeid RE, Hassan EA, Bettaieb F, et al (2015) Use of Cellulose and Oxidized Cellulose Nanocrystals from Olive Stones in Chitosan Bionanocomposites. Journal of Nanomaterials 2015:. https://doi.org/10.1155/2015/687490
[15] Rana AK, Frollini E, Thakur VK (2021) Cellulose nanocrystals: Pretreatments, preparation strategies, and surface functionalization. International Journal of Biological Macromolecules 182:1554–1581
[16] El-Wakil NA, Hassan EA, Abou-Zeid RE, Dufresne A (2015) Development of wheat gluten/nanocellulose/titanium dioxide nanocomposites for active food packaging. Carbohydrate Polymers 124:337–346. https://doi.org/10.1016/j.carbpol.2015.01.076
[17] Hassan ML, Abou-Zeid RE, Fadel SM, et al (2014) Cellulose nanocrystals and carboxymethyl cellulose from olive stones and their use to improve paper sheets properties. International Journal of Nanoparticles 7:261–277. https://doi.org/10.1504/ijnp.2014.067613
[18] Šturcová A, Davies GR, Eichhorn SJ (2005) Elastic modulus and stress-transfer properties of tunicate cellulose whiskers. Biomacromolecules 6:1055–1061. https://doi.org/10.1021/bm049291k
[19] Rusli R, Eichhorn SJ (2008) Determination of the stiffness of cellulose nanowhiskers and the fiber-matrix interface in a nanocomposite using Raman spectroscopy. Applied Physics Letters 93:. https://doi.org/10.1063/1.2963491
[20] Turbak A F, Snyder F W SKR (1983) Microfibrillated cellulose,a new cellulose product:properties,uses,and commercial potential. Journal of Applied Polymer Science 37:169
[21] Nagarajan KJ, Balaji AN, Ramanujam NR (2019) Extraction of cellulose nanofibers from cocos nucifera var aurantiaca peduncle by ball milling combined with chemical treatment. Carbohydrate Polymers 212:312–322. https://doi.org/10.1016/j.carbpol.2019.02.063
[22] Abdul Khalil HPS, Davoudpour Y, Islam MN, et al (2014) Production and modification of nanofibrillated cellulose using various mechanical processes: A review. Carbohydrate Polymers 99:649–665
[23] Spinu M, Dos Santos N, Le Moigne N, Navard P (2011) How does the never-dried state influence the swelling and dissolution of cellulose fibres in aqueous solvent? Cellulose 18:247–256. https://doi.org/10.1007/s10570-010-9485-8
[24] Almasi H, Ghanbarzadeh B, Dehghannia J, et al (2015) Heterogeneous modification of softwoods cellulose nanofibers with oleic acid: Effect of reaction time and oleic acid concentration. Fibers

and Polymers 16:1715–1722. https://doi.org/10.1007/s12221-015-4294-1

[25] Huang L, Zhao H, Yi T, et al (2020) Preparation and Properties of Cassava Residue Cellulose Nanofibril/Cassava Starch Composite Films. Nanomaterials 10:755. https://doi.org/10.3390/nano10040755

[26] Mendoza DJ, Hossain L, Browne C, et al (2020) Controlling the transparency and rheology of nanocellulose gels with the extent of carboxylation. Carbohydrate Polymers 245:116566. https://doi.org/10.1016/j.carbpol.2020.116566

[27] De France K, Zeng Z, Wu T, Nyström G (2020) Functional Materials from Nanocellulose: Utilizing Structure–Property Relationships in Bottom-Up Fabrication. Advanced Materials 2000657. https://doi.org/10.1002/adma.202000657.

[28] Abouzeid, R. E., Abd El-Kader, A. H., Salama, A., Fahmy, T. Y., & El-Sakhawy, M. (2022). PREPARATION AND PROPERTIES OF NOVEL BIOCOMPATIBLE PECTIN/SILICA CALCIUM PHOSPHATE HYBRIDS. CELLULOSE CHEMISTRY AND TECHNOLOGY, 56(3-4), 371-378.

[29] Hassan, M. L., Berglund, L., Abou Elseoud, W. S., Hassan, E. A., & Oksman, K. (2021). Effect of pectin extraction method on properties of cellulose nanofibers isolated from sugar beet pulp. Cellulose, 28, 10905-10920.

[30] Chuayplod, P., & Aht-Ong, D. (2018). A study of microcrystalline cellulose prepared from parawood (Hevea brasiliensis) sawdust waste using different acid types. Journal of Metals, Materials and Minerals, 28(2).

[31] Wai, W. W., Alkarkhi, A. F., & Easa, A. M. (2010). Effect of extraction conditions on yield and degree of esterification of durian rind pectin: An experimental design. Food and Bioproducts Processing, 88(2-3), 209-214.

[32] M. El-Sakhawy, K. Samir, A. Salama, and H. S. Tohamy, Cellul. Chem. Technol., vol. 52, pp. 193–200, 2018.

[33] Siqueira G, Bras J, Dufresne A (2010) Cellulosic bionanocomposites: A review of preparation, properties and applications. Polymers 2:728–765

[34] Abou-Zeid RE, Diab MA, Mohamed SAA, et al (2018) Surfactant-assisted poly(lactic acid)/cellulose nanocrystal bionanocomposite for potential application in paper coating. Journal of Renewable Materials 6:394–401. https://doi.org/10.7569/JRM.2017.634156.

[35] Trache, D., Hussin, M. H., Chuin, C. T. H., Sabar, S., Fazita, M. N., Taiwo, O. F., ... & Haafiz, M. M. (2016). Microcrystalline cellulose: Isolation, characterization and bio-composites application—A review. International Journal of Biological Macromolecules, 93, 789-804.

[36] Hasanin, M. S., Kassem, N., & Hassan, M. L. (2021). Preparation and characterization of microcrystalline cellulose from olive stones. Biomass Conversion and Biorefinery, 1-8.

[37] Zugenmaier P (2008) Crystalline cellulose and derivatives: characterization and structures. Springe.

[38] Hassan M, Abou-Zeid R, Hassan E, et al (2017) Membranes based on cellulose nanofibers and activated carbon for removal of Escherichia coli bacteria from water. Polymers 9:. https://doi.org/10.3390/polym9080335

[39] Hassan M, Hassan E, Fadel SM, et al (2018) Metallo-Terpyridine-Modified Cellulose Nanofiber Membranes for Papermaking Wastewater Purification. Journal of Inorganic and Organometallic Polymers and Materials 28:439–447. https://doi.org/10.1007/s10904-017-0685-7.

[40] Abou-Zeid RE, Diab MA, Mohamed SAA, et al (2018) Surfactant-assisted poly(lactic acid)/cellulose nanocrystal bionanocomposite for potential application in paper coating. Journal of Renewable Materials 6:394–401. https://doi.org/10.7569/JRM.2017.634156.

[41] Spinacé, M. A., Lambert, C. S., Fermoselli, K. K., & De Paoli, M. A. (2009). Characterization of lignocellulosic curaua fibres. Carbohydrate Polymers, 77(1), 47-53.